Title	Comparison of diesel spray with small injection amount between single-hole and multi-hole injectors: Results under same rail pressure and similar injection rate
Author(s)	Jin, Yu; Kim, Jaeheun; Kakami, Shinichi; Nishida, Keiya; Ogata, Yoichi; Luo, Hongliang
Citation	International Communications in Heat and Mass Transfer , 118 : 104862
Issue Date	2020-09-07
DOI	10.1016/j.icheatmasstransfer.2020.104862
Self DOI	
URL	https://ir.lib.hiroshima-u.ac.jp/00051515
Right	© 2020. This manuscript version is made available under the CC-BY-NC-ND 4.0 license http://creativecommons.org/licenses/by-nc-nd/4.0/ This is not the published version. Please cite only the published version. この論文は出版社版ではありません。引用の際には出版社版をご確認、ご利用ください。
Relation	

Comparison of Diesel Spray with Small Injection Amount between Single-hole and Multi-hole Injectors: Results under Same Rail Pressure and Similar Injection Rate

Yu Jin [1], Jaeheun Kim [1,2], Shinichi Kakami [1,3], Keiya Nishida [1], Yoichi Ogata [1], Hongliang Luo [1*]

1. University of Hiroshima, 1-4-1 Kagamiyama, Higashi-Hiroshima, Japan

2. Hyundai Kia Namyang R&D Center, Hwaseong, Korea

3. Honda Motor Co., Ltd. 2-1-1, Minami-Aoyama, Minato-ku, Tokyo, Japan

Abstract

A comparison of diesel spray for injectors with single-hole (SH) and multi-hole (MH) nozzles has been conducted under same rail pressure and similar injection rate (30 MPa for SH and 100 MPa for MH) conditions. The result showed that the spray of SH injector has a longer penetration under same rail pressure condition caused by the faster build-up process of sac pressure. The spray of MH injector has a larger spray angle resulted from the complicated nozzle flow. These further affect the evaporation rate and mixture formation process. Regarding the same rail pressure condition, the spray of SH injector shows a fast evaporation rate, as well as the MH injector, although the spray angle of SH injector is quite small. For the entire mixture formation process, more spray vapor of SH is distributed in the thin area. For similar

injection rate condition, the effect of different spray tip penetration can be eliminated while the advantage of the large spray angle of MH injector becomes apparent. The evaporation rate and mixture formation process of the SH injector are much worse than those of the MH injector. The complex nozzle internal flow of MH injector is responsible.

Keywords: Diesel; Spray; Single-hole; Multi-hole; Evaporating

1. Introduction

The spray behavior and mixture formation process in the engine cylinder play a decisive role in diesel engines. Since emission formation and engine performance are mainly controlled and determined by mixture status. Various research activities have been carried out on diesel spray for the common-rail injectors.

There are many visualization methods can be used to obtain the spray behavior. The most general method is to fix the injectors into a vessel (or constant volume chamber). The fuel is injected into the vessel which with the pre-defined ambient pressure and temperature. A single-hole (SH) injector has been widely used for experimental research, since it has a better optical observation and comprehensive study. In additional, the independent effects of the individual parameters are much easier to be clarified. Since the spray plume of SH injectors does not have the issues of optical path blocking and adjacent plume interference.

However, in a real engine, the injectors widely used are MH ones. Therefore, it is necessary to make sense of the difference of sprays between SH and MH types. Different nozzle flow characteristics inside sac are one of the crucial reasons lead to the spray behavior significantly different, especially when the needle lift is very low. The holes of SH injectors are located at the end of nozzle. Nevertheless, the holes of MH injectors are located at the side of the sac. The studies have shown that, nozzle flow state is directly linked with the location of the holes relative to the sac. [(1),(2)] besides, nozzle flow can be altered by needle lift dramatically.[(3)–(7)] The flow streamline inside nozzle is determined by needle lift. Initially, a low needle lift usually guides the flow into the sac directly. Then, fuel flows into the hole inlet from sac. Compared with SH injectors, a higher radial direction velocity can be created by the vortex formed inside the holes of MH injectors. As a result, MH injector has a larger spray angle caused by higher radial velocity.

The comparison between SH and MH injectors has been conducted by various studies under quasi-steady state conditions;[(8)–(9)] few studies concentrate on the spray with transient variation, such as low needle lift and small injection mount cases. It is also very important to investigate the spray behavior under quite small injection amount, since small injection amount represent the sprays of pilot injected fuel of a real engine. Because of the greatly influences of low needle lift on the upstream flow state of holes, it is meaningful to conduct a comparison of mixture formation process between SH and MH injectors. Prior to the small injection amount, a comparison had been conducted for the quasi-steady spray (large injection amount) and has been published in SAE World Congress 2019.[10]

The pressure-drop between the sac volume and the ambient gas actually controlled by the exit velocity. The pressure build-up process of sac volume for SH and MH injectors would be different under same rail pressure condition. That is caused by the different flow rates and areas of SH and MH injectors. Therefore, in addition to the contents mentioned above, the injection pressure of the SH injector was adjusted accordingly to match the injection rate of both injectors equal. The influence of the difference of the sac pressure can then be negligible between two injectors. The mixture formation process was analyzed again under such condition, as well as the nozzle internal flow and near-field spray simulation. Then, another comparison of spray behavior of both injectors under different injection control parameters can be conducted. This can further provide an insight into priority of the controlling parameters when conducting experiments with an SH injector as the substitute of a MH injector.

2. Investigation Method

2.1 LAS Principle and experimental setup

The different attenuation between visible (Vis) and ultraviolet (UV) light is the basic principle of the Laser Absorption and Scattering (LAS) technic. Therefore, we can obtain the concentration of vapor and liquid phases by comparing the attenuation of Vis and UV lights. The UV light intensity can be attenuated by both the vapor and liquid phases. The attenuation of liquid phase is caused by droplet scattering and absorption. The attenuation of vapor phase is caused by vapor absorption. While, the attenuation of Vis light is only caused by the droplet (liquid phase) scattering. This phenomenon could be expressed by the Eqs. (1) and (2), respectively:

$$\log{(I_0/I_t)_{\lambda_A}} = \log{(I_0/I_t)_{L_{sca}}} + \log{(I_0/I_t)_{L_{abs}}} + \log{(I_0/I_t)_{V_{abs}}} \quad (1)$$

$$\log{(I_0/I_t)_{\lambda_T}} = \log{(I_0/I_t)_{L_{sca}}} \quad (2)$$

where $\log{(I_0/I_t)_{\lambda_A}}$ and $\log{(I_0/I_t)_{\lambda_T}}$ are the total optical thickness of UV and visible lights, which represent the attenuation of each light intensity. $\log{(I_0/I_t)_{L_{sca}}}$, $\log{(I_0/I_t)_{L_{abs}}}$ and $\log{(I_0/I_t)_{V_{abs}}}$ represent the attenuation caused by the droplet scattering, droplet absorption and vapor absorption. Since $\log{(I_0/I_t)_{L_{abs}}}$ can be ignored in Eq. (1). Therefore, vapor absorbance can be calculated by Eq. (3):

$$\log{(I_0/I_t)_{V_{abs}}} = \log{(I_0/I_t)_{\lambda_A}} - \log{(I_0/I_t)_{\lambda_T}} \quad (3)$$

The experimental setup schematic is showed in Figure 1. Two Charge Coupled Device (CCD) cameras and a pulsed ND-YAG laser are used for the optical system. The wavelength of 266 nm and 532 nm are used for UV and Vis, respectively. Firstly, The UV and Vis lights are expanded to the size similar with the optical window (quartz) of the chamber. Then, merged lights pass through the spray inside the chamber. Subsequently, the lights, which have been attenuated by the spray, are separated again by a light splitter and captured by CCD cameras. The mass distributions and equivalence ratios of vapor and liquid phases can be analyzed base on vapor and liquid absorbance by employing Bouguer-Lambert-Beer's law[11]. More details of LAS technic can be found in previous literatures. [(12)–(14)]

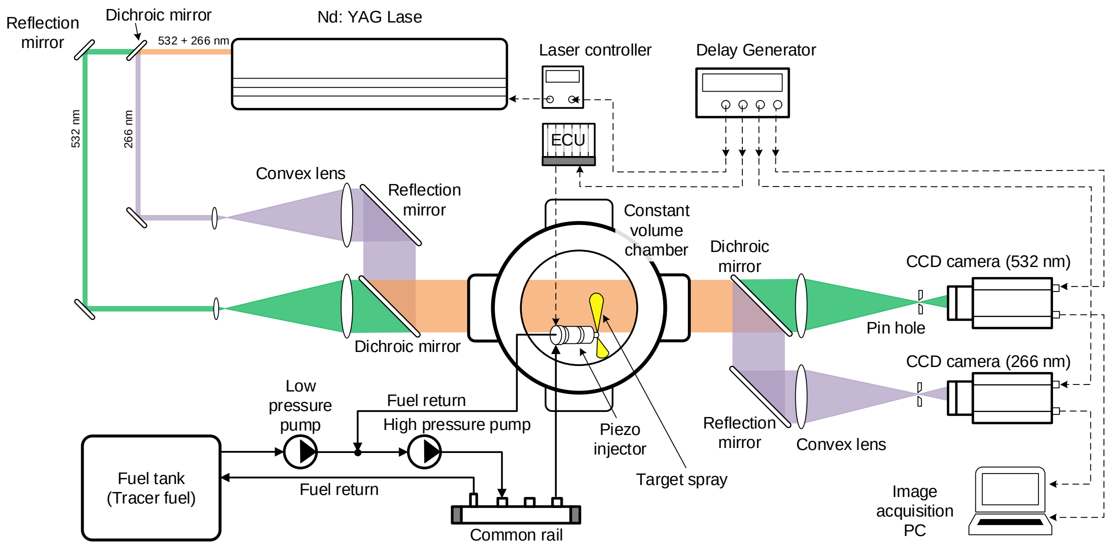

Figure 1 Schematic of experimental setup

A blended fuel (tracer fuel) of α-methyl-naphthalene (2.5%) and n-tridecane (97.5%) is used in the experiment. The physical properties of tracer fuel are listed in Table 1. The tracer fuels selection and its requirements for LAS technic can be found in previous literature[12].

Table 1 Properties of the test fuel

Items	Blended fuel α-MN (2.5%), n-tridecane (97.5%)
Density [kg/m^3]	767
Boiling point [K]	509
Kinematic viscosity [mm^2/s]	2.48

For one injection event, with the aim of reducing the noises during the image processing, an interval of 0.5 sec were set between images of background and spray. The injection interval and the imaging timings were controlled by a delay generator. The imaging moments were determined by this interval during one injection event. Table 2 list the specification of the injectors adopted in this work. The nozzles of two injectors have identical geometry, except that the umbrella angle (included angle) for the MH injector is 155 degrees. In order to obtain the sprays that the spray axis parallel to the imaging plane, the chamber cover was carefully designed for MH injector (Figure 2). The MH injector is tilted 45° and arranged eccentrically on the top of the cover. The target spray (parallel to imaging plane) has an angle of 17.2° with horizontal plane. Unfortunately, as the observation issues for MH injector mentioned previously, the area within 9mm of the hole exit is invisible.

Table 2 The injectors specification

Items	SH	MH
Type of injector [-]	Piezo-type	
holes Number [-]	1	7
Hole diameter at exit [mm]	0.123	
Hole length [mm]	0.8	
K-factor [-]	2.7	
Umbrella angle [deg.]	-	155

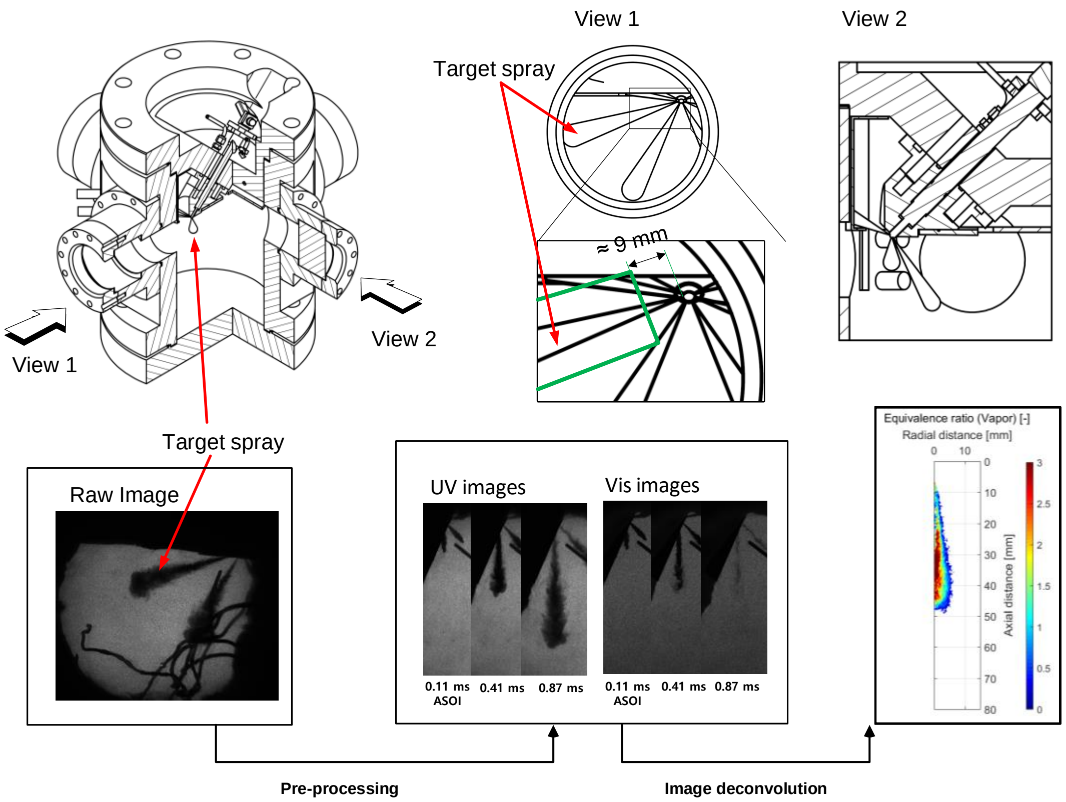

Figure 2 The multi-hole injector arrangement for axisymmetric spray, and the sequence for image-processing

Table 3 summarized the experimental conditions. For better understanding, the injection amounts have been normalized to the mass injected per hole throughout this paper. A typical condition in-cylinder with a high temperature and low density was selected for the ambient condition at the end of compression stroke. The aim of selecting this condition is to simulate the vicinity injection condition at the pilot timing. For the same rail pressure condition, the rail pressure and injection amount were 100 MPa and 0.5 mg/hole, respectively. For similar injection rate condition, the rail pressure of the SH injector was adjusted to 30 MPa to achieve a similar injection rate as the MH injector.

Table 3 Experimental conditions

Items	SH	MH
Ambient pressure [MPa]	2.0	
Ambient density [kg/m^3]	8.4	
Ambient temperature [K]	800	
Same rail pressure		
Injection amount [mg/hole]	0.5	
Rail pressure [MPa]	100	
Similar injection rate		
Injection amount [mg/hole]	0.53	0.59
Rail pressure [MPa]	30	100

2.2 Numerical setup of CFD simulation

In the simulation section, two simplified nozzles which have same nozzle tip geometries with the experiment section were employed for analyzing the flow state inside the holes of nozzle and near-field behavior. As shown in Figure 3, the entire nozzle tip is modeled for the SH injector, while one-seventh (one hole) of the nozzle tip is selected for MH injector. In addition, a cylindrical cavity with a length of 1.5 mm and a radius of 3 times the hole diameter is set at each hole exit to maintain a stable ambient pressure.

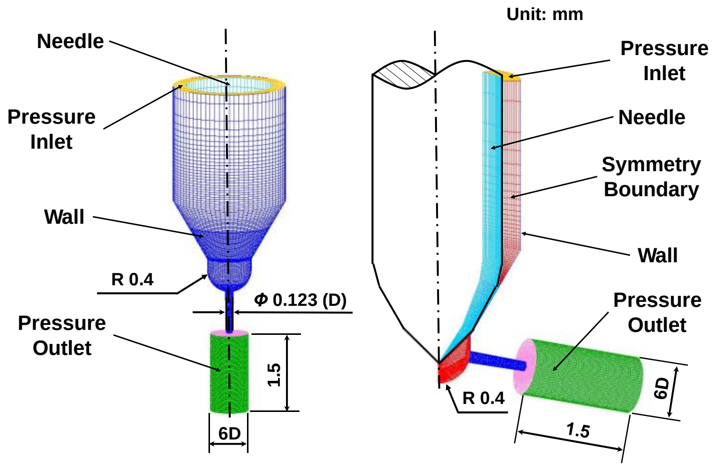

Figure 3 Nozzle structure, meshes and boundary conditions

Commercial software AVL Fire (Ver. 2014) was employed for this numerical calculation. The fluids property, boundary conditions and models are summarized in Table 4. The ambient condition and injection pressure of simulation are same with the experiment for similar injection rate. The four-equation model k-ζ-f of RANS method and multi-fluid model are selected as the turbulence and multiphase flow model, respectively. The Linear Cavitation model based on Rayleigh equation(15) is adopted for depicting the cavitating flow, and its Mass Exchange is described below:

$$\Gamma_v = \rho_l N 4\pi R^2 \dot{R} = -\Gamma_l \quad (4)$$

where N represent bubble number density, R represent bubble radius, v is vapor phase (diesel vapor) and l is liquid phase (diesel).

Table 4 Fluids property, conditions and models in simulation

Items	SH	MH
Commercial software	AVL Fire (Ver. 2014)	

Diesel	Density (kg/m^3)	830	
	Viscosity ($N \cdot s/m^2$)	0.00214	
Vapor	Density (kg/m^3)	7	
	Viscosity ($N \cdot s/m^2$)	10^{-5}	
Air	Density (kg/m^3)	17.4	
	Viscosity ($N \cdot s/m^2$)	1.8×10^{-5}	
	Inlet Pressure (MPa)	30	100
	Outlet Pressure (MPa)	0.75	
	Temperature (K)	300	
	Turbulence Model	k-ζ-f	
Cavitation Model	Linear Cavitation Model	-	
	Cavitation Bubble Density	1.0×10^{12}	
	Saturated Vapor Pressure (Pa)	892	
Needle-holder gap (μm)		2	
Cell size around the hole (μm)		2.7	2.6

3. Results and discussions

3.1 Evaporating spray characteristics

For better understand the experimental content of this paper, the authors would like to show the injection rate of SH and MH injectors under both same rail pressure and similar injection rate conditions (Figure 4) firstly. The injection rate profiles were measured by ONO SOKKI FJ7000 Injection Measuring System which is based on Zeuch's method.[16],[17][17]

As shown in Figure 4(a), The injection rate curve of SH injector increased much faster than that of MH injector during the rising period. This implies that the SH injector has a larger exit velocity, which makes the spray parameters of injectors greatly different.

In order to eliminate the impact of the exit velocity on spray characteristics, authors achieved a similar exit velocity magnitude of the SH and MH injectors by adjusting the rail pressure, and got the injection rate profiles as shown in Figure 4(b). The rail pressure of SH injector is 30 MPa, and that of MH injector is 100 MPa.

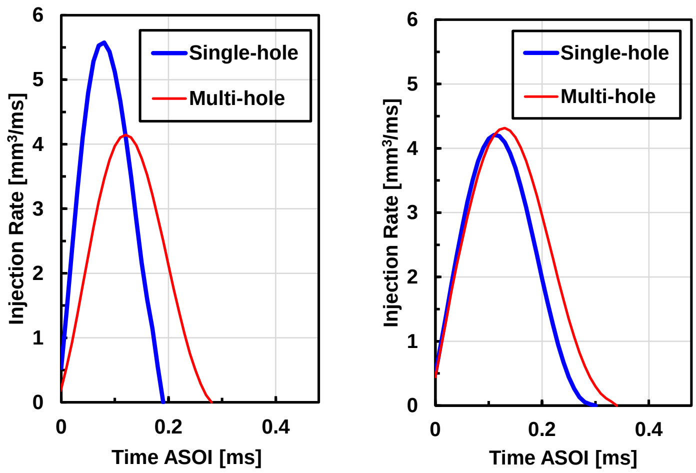

(a) Same rail pressure of 100MPa (b) Similar injection rate

Figure 4 Injection rate.

Before the discussion of spray characteristics, the authors first focus on two definitions of spray parameters, which are very important and fundamental parameters that directly represent spray diffusion and fuel-air mixing processes (Figure 5). Spray tip penetration S is defined as the length from nozzle tip to spray tip. The angle ∠AOB names spray angle is defined as the angle between the nozzle tip and the spray boundary at the half S.

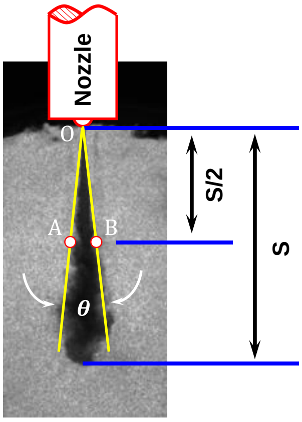

Figure 5 Spray tip penetration and spray angle definitions.

Figure 6 shows the spray tip penetration of the SH and MH injectors under both same rail pressure and similar injection rate conditions. Due to the smaller total exit cross-sectional area (one-seventh of the MH injector), the sac pressure of SH injector increases significantly faster, which leads to a larger velocity at the hole exit of SH injector. This is why the SH injector has a larger spray tip penetration, which would lead to more air entrainment. As for the similar injection rate condition, the spray tip penetrations for SH and MH injectors show a great coordination before the end of injection caused by the similar injection rate and exit velocity.

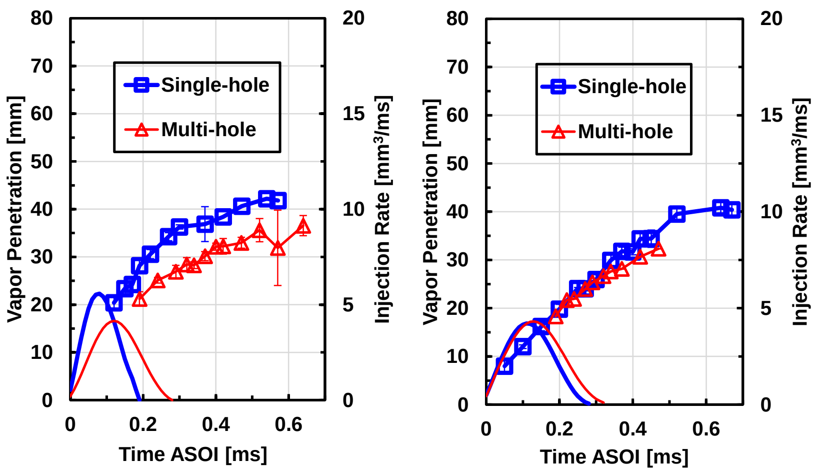

(a) Same rail pressure of 100MPa (b) Similar injection rate

Figure 6 Spray tip penetration (vapor) under same rail pressure of 100 MPa and Similar injection rate.

For a certain diesel injector, as we all know, spray angle and tip penetration mainly determined by the rail pressure and ambient density. Generally, the faster the spray tip penetration increases, the smaller the spray angle is under the constant ambient condition. While for diverse types of injectors, the situation will be quite different since difference existing in various parameters, such as hole geometry, hole location, sac volume, and needle tip geometry. In the comparison of SH and MH, both the hole location and the total sectional area of holes were taken into consideration. Obviously, as shown in Figure 7(a), the spray of SH injector has a much smaller spray angle. Of course, the faster hole exit and spray tip velocities made a lot of contributions on it. However, if we shift our focus to the similar injection rate condition, we can find a similar scene in Figure 7(b). The spray angles of the SH and the MH injectors still maintains a large gap. As described above, SH and MH injectors have similar injection rate, exit velocity and spray tip penetration. That means hole location has a greater impact on spray angle than spray tip penetration (exit velocity). Therefore, nozzle internal flow plays a significant role on spray angle and will be further discussed in simulation section.

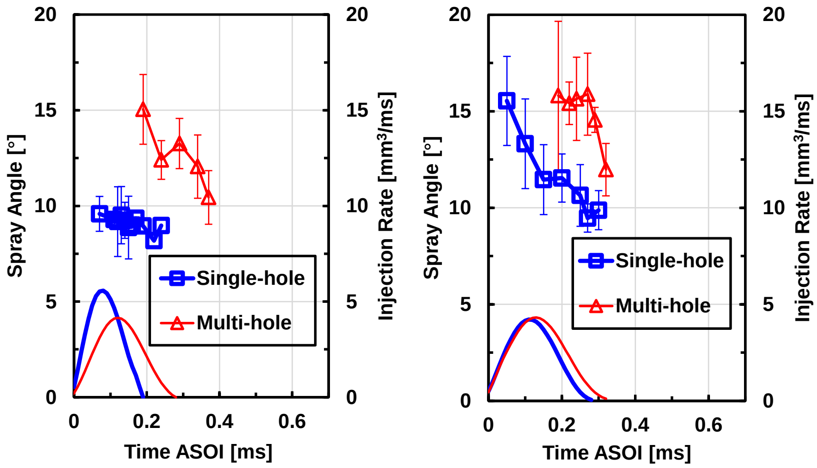

(a) Same rail pressure of 100MPa (b) Similar injection rate

Figure 7 Spray angle.

It is well known that equivalence ratio, as a crucial factor of combustion process, is an extremely important indicator of engine performance and exhaust emission. With the rise of new combustion modes such as HCCI and PCCI, the requirements for the equivalence ratio of mixture formation and combustion process are becoming higher and higher. Both excessively rich and lean mixtures would be likely to cause undesired situations during engine operation. However, the difference between the equivalence ratio of SH and MH injector is not clear at present. It is not appropriate to apply the experimental results of the SH injector to the real engine. Therefore, the following of this article will mainly focus on the equivalence ratio of SH and MH injectors.

Figures 8 and 9 show the spray equivalence ratio distributions for the two injectors under same rail pressure and similar injection rate conditions, respectively. The right side of each spray picture represents the vapor phase and the other side is the liquid phase. As described in Figure 2, the spray of MH injector has an invisible area near the nozzle tip. As for the same rail pressure condition, the equivalence ratio distribution of spray for SH and MH injectors shows a similar tendency versus time when the end of injection (EOI) is set as time zero, no matter the moment is after the end of injection (AEOI) or before the end of injection. However, for the similar injection rate condition, a completely different scenario is presented. The spray of the MH injector has a large amount of mass evaporated (the red spray center) before the end of injection, while that of the SH injector still has a very high liquid concentration at 0.05ms AEOI around the spray center. The spray equivalence ratio of MH injector has become very low due to more gas entrainment and vapor diffusion at 0.20ms AEOI. However, the spray center of SH injector (vapor phase) is still red (high concentration and equivalence ratio), and even a small amount of liquid fuel exists. In other words, the time required to form a homogeneous mixture is a very noteworthy issue when the mixture formation of an SH injector is analogous to a MH injector.

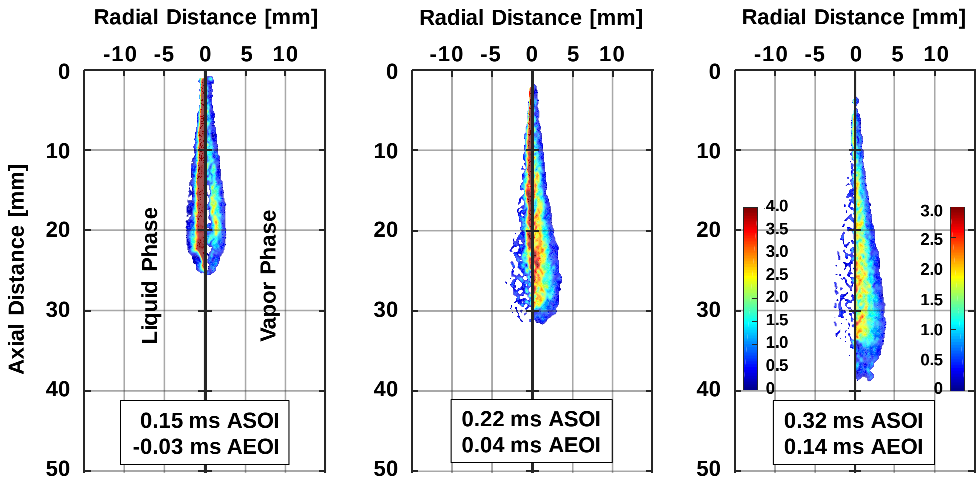

(a) Single-hole injector

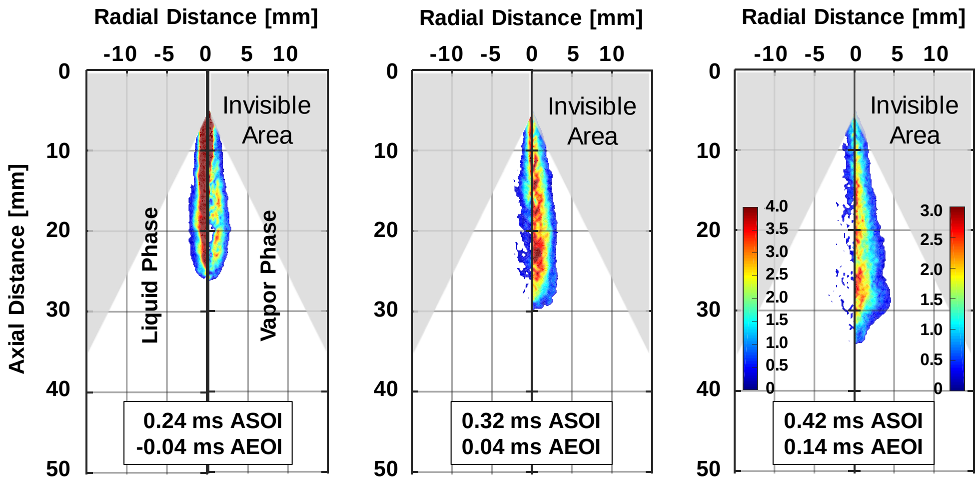

(b) Multi-hole injector

Figure 8 Equivalence ratio distribution under same rail pressure of 100 MPa.

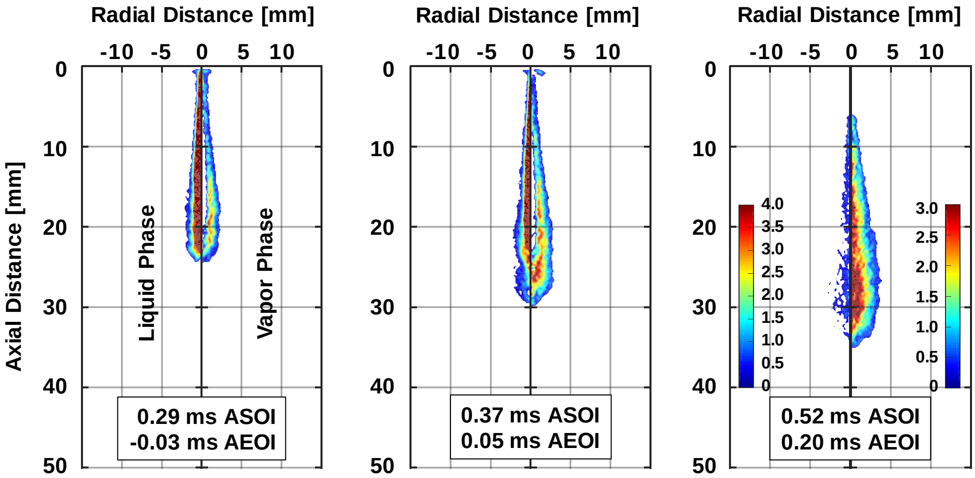

(a) Single-hole injector

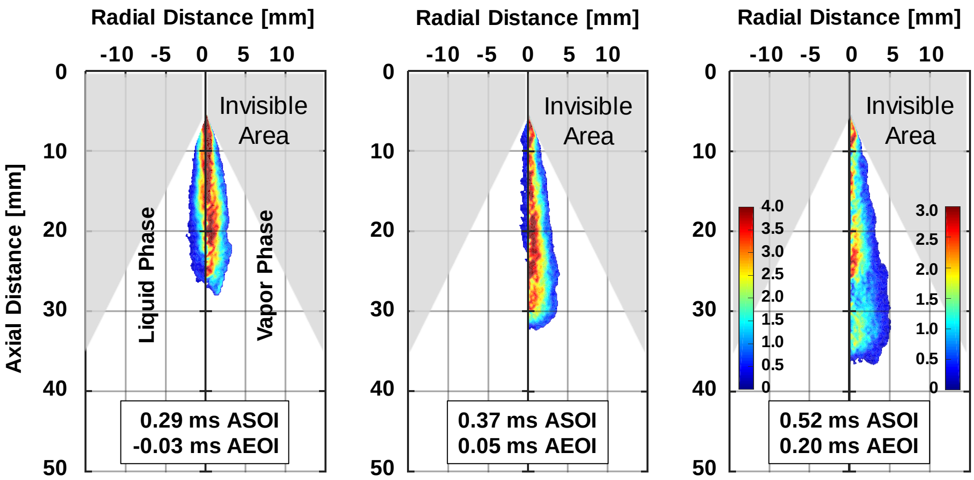

(b) Multi-hole injector

Figure 9 Equivalence ratio distribution under similar injection rate profile.

The three-dimensional average was performed for the equivalence ratio distributions, and the variation curves of the spatial average (mean equivalence ratio) over time were obtained as shown in Figure 10. The mean equivalence ratio peaks of both SH and MH injectors seem to appear near the end of injection under same rail pressure condition, but the peak of SH injector appears to occur slightly later than the end of injection. That means the equilibrium between air entrainment and fuel evaporation occurs near the end of injection. Besides, we noticed that the mean equivalence ratio of the MH injector is much larger than that of the SH injector. This should be due to the faster evaporation rate or lesser air entrainment of the MH injector. We will further explore the reasons when discussing the evaporation rate.

As for similar injection rate condition, the peak of mean equivalence ratio for the SH injector obviously appears very late, about 0.2 ms AEOI (0.5 ms ASOI), where that of MH injector has dropped to an extra low level. That reveals the spray of SH injector has a quite low evaporation rate during the injection period. To illuminate this result, we pulled out the mass of vapor production and entrained ambient gas under similar injection rate condition (Figure 11). Obviously, the vapor production of MH injector is more than twice of SH injector before the end of injection, even though the disparity of entrained ambient gas has no such large gap. There must be other factors that make a big difference in the atomization process. It shows that the influence of internal flow of nozzle on its atomization cannot be underestimated.

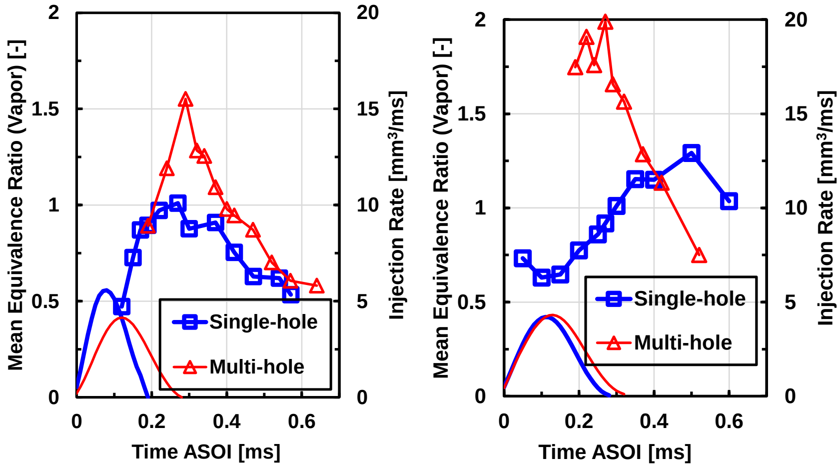

(a) Same rail pressure of 100MPa (b) Similar injection rate

Figure 10 Mean equivalence ratio.

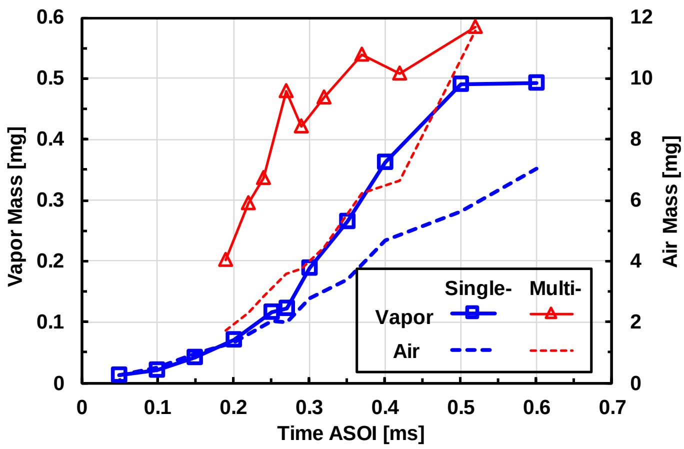

Figure 11 Vapor production and entrained ambient gas under similar injection rate condition.

Figure 12 shows the evaporation ratio versus time which is based on ASOI for the sprays of the two injectors. As for the same rail pressure condition showed in Figure 12(a), the evaporation ratio of SH and MH injectors show a similar trend. Therefore, the evaporation ratio is not the reason why the MH injector has a larger equivalence ratio which was discussed in Figure 10. Then there is only one crucial reason (less entrained gas mass) left for the larger equivalence ratio of MH injector. That is to say, although the spray angle of MH injector is larger, the longer spray tip penetration of the SH spray can make up for the loss in mixture volume caused by small spray angle. As for similar injection rate condition, the spray of SH injector shows a quite slower evaporation ratio comparing with that of MH injector. The spray angle (or spray volume) is one of the most important reasons for that. In addition, as mentioned above, the effect of nozzle flow on the atomization process is also very important.

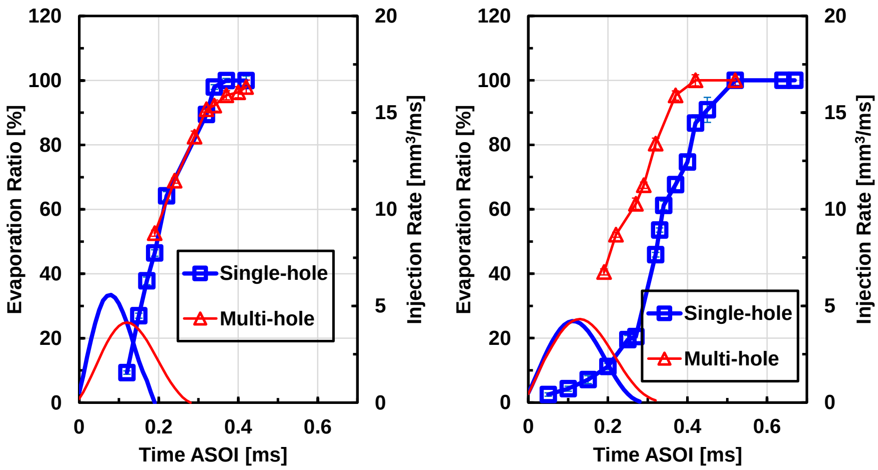

(a) Same rail pressure of 100MPa (b) Similar injection rate

Figure 12 Evaporation ratio.

All in all, our ultimate goal is to form a high-quality mixture to improve combustion efficiency and reduce emissions. The relationship between mixture concentration (equivalence ratio) and time (crank angle) is extremely important, which will to a large extent affect the heat release rate of combustion and indicated efficiency. Hence, the vapor mass distribution versus equivalence ratio at different instants should be considered very circumspect. As shown in Figure 13 (a), most fuel vapor of SH injector is distributed in the region where the equivalence ratio is less than 2 after the end of injection. However, 60% of the fuel vapor in MH injector is located in the region where the equivalence ratio larger than 2 at the end of injection and dispersed to the low concentration region rapidly. Although the tendency of vapor concentration looks absolutely different for two injectors, the region with high vapor concentration of MH injector quickly disappeared, which may have little effect on soot emission in the combustion process. Further combustion experiment is required to get the final conclusion. As for the similar injection rate condition, there is no doubt that the vapor mass distribution of MH injector shows the same scene with the same rail pressure condition. In contrast, the spray of SH injector still has more than 30% vapor distributed in the high concentration region (equivalence ratio greater than 2) 0.20 ms AEOI. The slower evaporation rate is one of the reasons. Nevertheless, lower dispersion rate, caused by the lower turbulence kinetic energy and lower radial velocity, should be a more influential factor, which will be discussed later.

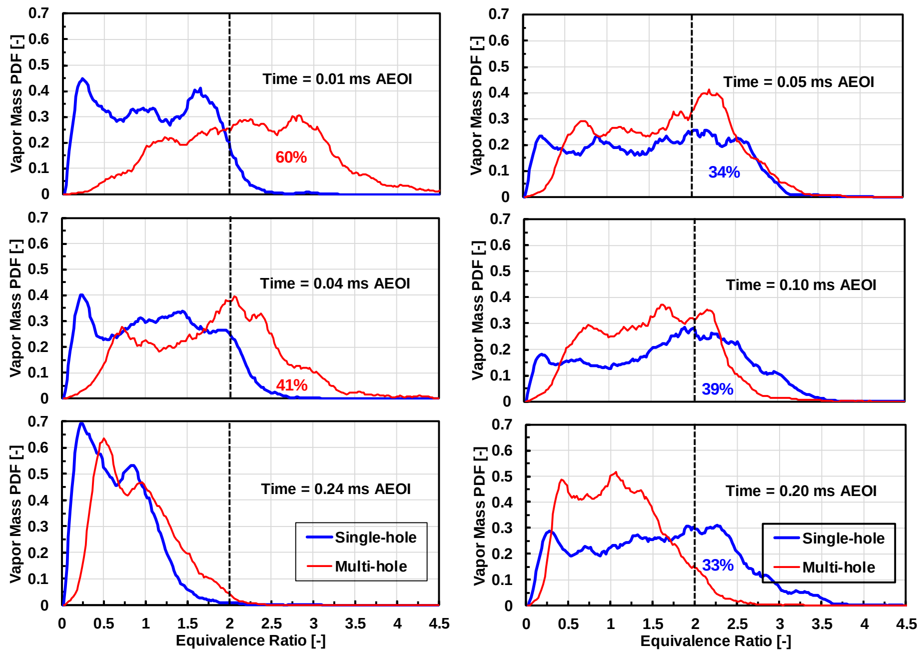

(a) Same rail pressure of 100MPa (b) Similar injection rate

Figure 13 Vapor mass distribution with equivalence ratio.

3.2 Nozzle flow and near-field spray in CFD simulation results

As discussed above, the nozzle internal flow plays a crucial role in spray and mixture process, and indirectly affects the combustion process and emissions. In order to better interpret the phenomena found in the experiment section, the internal and near-field flow simulation of the SH and MH nozzles has been conducted for similar injection rate condition. Figure 14 shows the needle lift curves used in nozzle flow simulation and the flow rate comparison between simulation and experiment. The needle lift curves were simplified from the X-Ray data of AIST (Advanced Industrial Science and Technology) which used the same type of injectors as well as the authors. Two moments (t_a and t_b) of flow rate curves were selected for subsequent discussion on flow characteristic under both needle rising and falling processes.

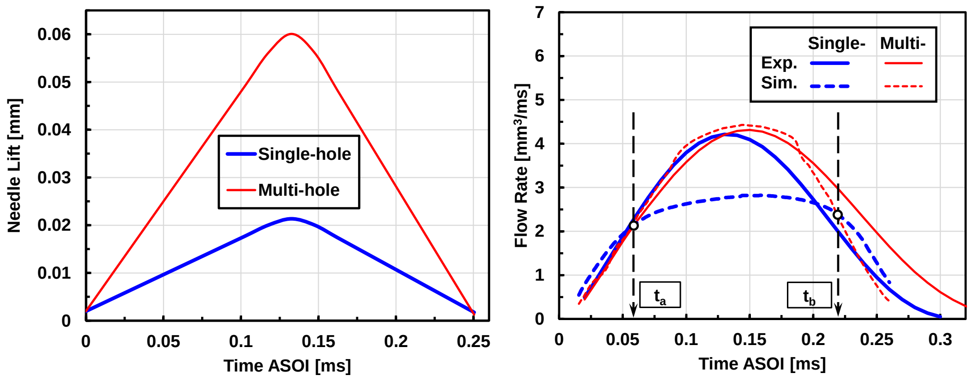

(a) Needle lift curve (b) Flow rate comparison with simulation

Figure 14 Needle lift in simulation and flow rate comparison.

To comprehend the content of following figures easily, Figure 15 shows the X, Y, Z coordinates at hole exit. The center of hole exit was selected as the origin of coordinates. The radial velocity magnitude and turbulence kinetic energy (TKE) at hole exit and 1mm downstream (Z = 1 mm) will be discussed in Figures 17, 18 and 19. The radial velocity is defined as vector sum of velocity compositions in X and Y directions, as shown in Eq. (5). The distance between the dashed lines shown in the figure is 0.125mm (hole diameter).

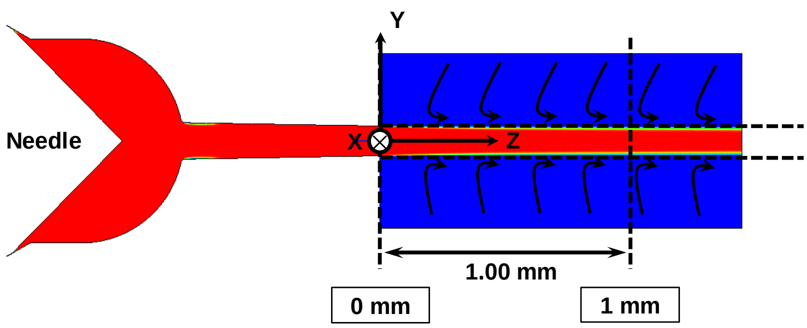

Figure 15 X, Y, Z coordinates at hole exit

$$\overrightarrow{v_r} = \overrightarrow{v_x} + \overrightarrow{v_y} \qquad (5)$$

Figure 16 shows the velocity vectors of longitudinal section along the holes. It is obviously that, no matter hole exit or other cross sections, both the vector direction and velocity magnitude inside the hole of SH nozzle are extremely uniform along the cross section (Y coordinate). Totally different from the SH nozzle, the velocity vectors have various features along both the hole axis (Z coordinate) and radial direction. This fascinating sight is even more evident in the radial velocity distributions at the hole exit (Figure 17). The sharp change in velocity direction of the hole is mainly caused by the backflow formed by the fluid entering the hole, which also leads to an inconformity in velocity magnitude of hole exit. This unique characteristic of MH nozzle can significantly increase the radial velocity of the spray, thereby promoting subsequent atomization and air entrainment.

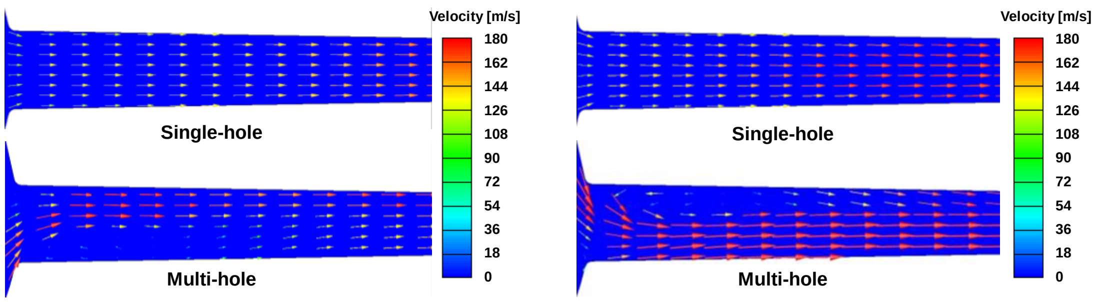

(a) Time = t_a (b) Time = t_b

Figure 16 Velocity distributions inside holes

The radial velocity vectors of SH and MH nozzles at the hole exit are shown in Figure

17. The radial velocity of MH exit is obviously higher than that of the SH during either the needle rising or falling period. Besides, two large vortexes occur inside the hole of MH nozzle, which were caused by the elbow-like structure, and will increase the TKE magnitude, improve the atomization process and enhance air entrainment. It is worth noting that the radial velocity peak of MH exit at t_b is significantly greater than that of t_a, even it shows the similar flow rate at the two moments in Figure 14(b). We all know that the total evaporation time should be connected with fuel injected at the moments near the end of injection. That is to say, for the MH injector, the large radial velocity at hole exit near the end of injection is an important reason for the faster evaporation rate.

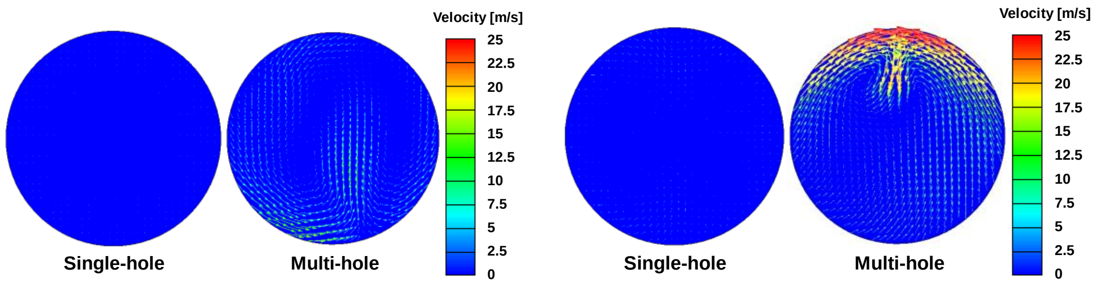

(a) Time = t_a (b) Time = t_b

Figure 17 Radial velocity distributions at hole exit

Figures 18 and 19 show the radial velocity and TKE magnitude along the horizontal and vertical lines at both the hole exit (Z = 0 mm) and 1 mm downstream (Z = 1 mm). As for MH injector, the horizontal line is defined base on the placement shown in

Figure 3. The radial velocity and TKE of air region which represent the air entrainment at Z = 1mm are also shown in the figures. Overall, no matter the radial velocity or TKE magnitude, the values of MH are much larger than that of SH at both hole exit and downstream. What is worth mentioning is that the large values in (or near) the hole axis of MH can great enhance the atomization process by promoting the liquid core breakup.

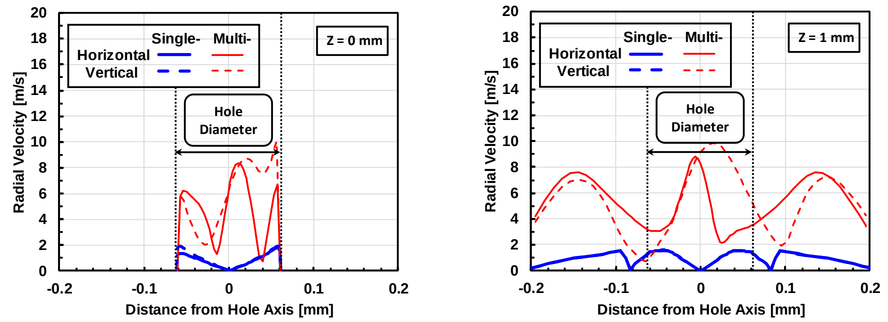

(a) Time = t_a

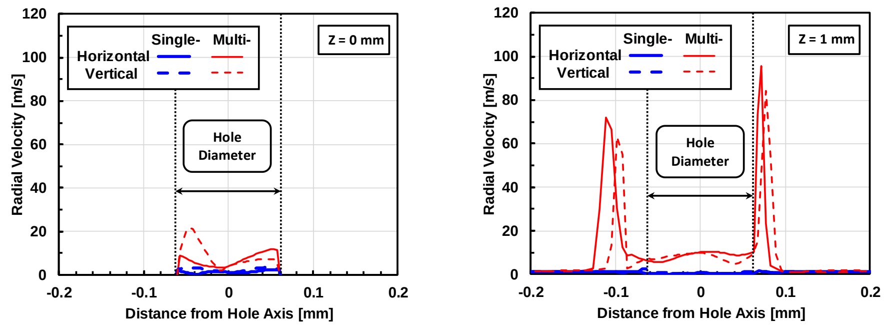

(b) Time = t_b

Figure 18 Radial velocity magnitude distributions along the horizontal (X) and vertical (Y) lines at Z = 0 mm and Z = 1 mm.

As mentioned before, the MH injector has a large spray angle under both the same rail pressure and similar injection rate conditions. The larger radial velocity and TKE must make a lot of contributions to spray angle. That is why the evaporation rate of MH injector can catch up with that of the SH injector under the same injection pressure. In addition, the evaporation rate of MH spray is much faster than that of SH under similar injection rate condition, which is closely related to the radial velocity and TKE of hole exit. That is beneficial to the formation of homogeneous mixtures, both spatially and temporally.

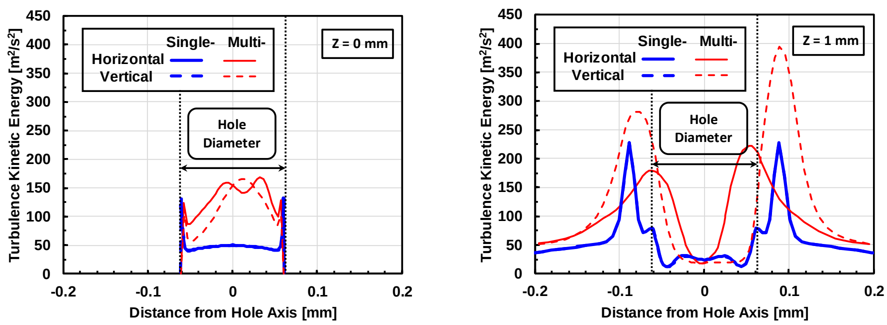

(a) Time = t_a

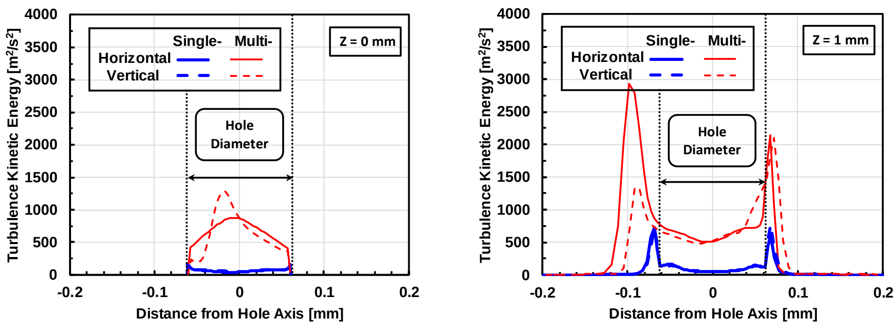

(b) Time = t_b

Figure 19 Turbulence kinetic energy distributions along the horizontal (X) and vertical (Y) lines at Z = 0 mm and Z = 1 mm.

Conclusions

A comparison on the mixture formation process of a fuel spray between single-hole (SH) and multi-hole (MH) injectors has been conducted. The laser absorption scattering (LAS) technic was performed to obtain the fuel equivalence ratio distributions of vapor and liquid phases. A blended fuel of α-MN and n-tridecane was used in the experiment. The spray evolution with small injection amount under same injection pressure (100 MPa for both injectors) or similar injection rate condition (30 MPa for SH injector, and 100 MPa for MH injector) were observed, respectively. Following conclusions can be made accordingly.

1. Under the same injection pressure condition, the vapor penetration of SH injector is greater than that of MH injector, due to the faster sac pressure build-up process.

2. MH injector has a larger spray angle than SH injector caused by the complex internal flow. The results of nozzle flow simulation show that there were greater portion of radial velocity term at the nozzle exit of MH injector at the transient period (low needle lift condition). This might have yielded a high spray angle for MH injector with small injection quantity, either under the same rail pressure or similar injection rate conditions.

3. The mixture formation of SH injector is slightly better than that of MH injector under same injection rate condition. The entire injection event of small injection

amount took place under the transient condition. The greater spray tip penetration caused by the faster sac pressure build-up process yielded greater air entrainment rate and amount for the SH injector. However, the difference in air entrainment rate and amount as a function of axial distance can be eliminated for both injectors under the same injection rate condition, since their vapor penetrations are similar to each other. The mixture formation process for SH injector then become worse than that of MH injector. The narrow spray angle and dense liquid core of the SH injector caused a lower evaporation ratio at the EOI timing. The overall equivalence ratio moves towards lean side for the MH injector as the time elapsed. However, since the SH injector no longer has any advantages on the vapor penetration, the evaporation rate is slow, and the mixture is not able to lean out quickly due to continuous portion of liquid core evaporating into vapor, maintaining the rich mixture. The mixture starts to lean out after when the vapor was fully evaporated.

4. Regarding the same injection pressure condition, the vapor penetration plays an important role in the evaporation rate and air entrainment, thus improved the lean mixture formation process, despite of the smaller spray angle of SH injector has. When the vapor penetration becomes similar (by means of controlling the injection pressure) for both injectors, the mixture formation becomes worse for SH injector as a result of the smaller spray angle and dense liquid core.

Acknowledgement

This work was supported by the Council for Science, Technology and Innovation (CSTI), Cross-ministerial Strategic Innovation Promotion Program (SIP), "Innovative combustion technology" (funding agency: JST).

References

(1) He, Z.; Zhong, W.; Qian, W.; et al. Effect of nozzle geometrical and dynamic factors on cavitating and turbulent flow in a diesel multi-hole injector nozzle. *Int. J. Therm. Sci*. **2013**, 70, 132−143.

(2) Farrar-Khan, J. R.; Andrews, G. E.; Williams, P. T.; et al. The influence of nozzle sac volume on the composition of diesel particulate fuel derived SOF. *SAE Tech. Pap. Ser.* **1992**.

(3) Zhong, W.; He, Z.; Wang, Q.; et al. Experimental study of flow regime characteristics in diesel multi-hole nozzles with different structures and enlarged scales. *Int. Commun. Heat Mass* **2014**, 59, 1-10.

(4) Salvador, F. J.; Martínez-López, J.; Caballer, M.; et al. Study of the influence of the needle lift on the internal flow and cavitation phenomenon in diesel injector nozzles by CFD using RANS methods. *Energ. Convers. Manage.* **2013**, 66, 246-256.

(5) Viera, J. P.; Payri, R.; Swantek, A. B.; et al. Linking instantaneous rate of injection to X-ray needle lift measurements for a direct-acting piezoelectric injector. *Energ. Convers. Manage.* **2016**, 112, 350-358.

(6) Baldwin, E.; T.; Grover, Jr. R. O.; Parrish, S. E.; et al. String flash-boiling in gasoline direct injection simulations with transient needle motion. *Int. J. Multiphas. Flow* **2016**, 87, 90-101.

(7) Tsunemoto, H.; Montajir, R. M.; Ishitani, H.; et al. The Influence of Pressure in the Nozzle Sac and Needle Lift on Fuel Spray Behavior and HC Emissions in DI Diesel Engines. *SAE Tech. Pap. Ser.* **1999**.

(8) Lai, M. C.; Zheng, Y.; Xie, X. B.; et al. Characterization of the near-field spray and internal flow of single-hole and multi-hole sac nozzles using phase contrast X-ray imaging and CFD. *SAE Int. J. Engines* **2011**, 4(1), 703-719.

(9) Dong, P.; Inaba, T.; Nishida, K.; et al. Characteristics of the internal flow and the near-field spray of a single-hole injector and a multi-hole injector for diesel engines. *P. I. MECH. ENG. D-J. AUT.* **2016**, 230(5), 632-649.

(10) Kim, J.; Kakami, S.; Jin, Y.; et al. Internal Fuel Flow, Near-Field and Far-Field Spray Evolution, and Mixture Formation Characteristics of Diesel Injectors-A Comparison between Multi-and Single-Hole Injectors. *SAE Tech. Pap. Ser.* **2019**.

(11) Bohren, C. F.; Huffman, D. R. Absorption and Scattering of Light by Small Particles.

Wiley Online Library, **1998**.

(12) Mamoru, S.; Nishida, K.; Hiroyasu H. Simultaneous concentration measurement of vapor and liquid in an evaporating diesel spray. *SAE Tech. Pap. Ser.* **1993**, 1164-1186.

(13) Zhang Y. A study on mixture formation in diesel sprays with split injection strategy. *Doctoral degree dissertation, Hiroshima University,* **2001**.

(14) Zhang, Y.; Nishida, K.; Yoshizaki, T. Quantitative measurement of droplets and vapor concentration distributions in diesel sprays by processing UV and visible images. *SAE Tech. Pap. Ser.* **2001**.

(15) Rayleigh, L. On the pressure developed in a liquid during the collapse of a spherical cavity. *The London, Edinburgh, and Dublin Philosophical Magazine and Journal of Science* **1917** 34(200), 94-98.

(16) Takamura, A.; Ohta, T.; Fukushima, S.; et al. A study on precise measurement of diesel fuel injection rate. *SAE Tech. Pap. Ser.* **1992**.

(17) Ikeda, T.; Ohmori, Y.; Takamura, A.; et al. Measurement of the Rate of Multiple Fuel Injection with Diesel Fuel and DME *SAE Tech. Pap. Ser.* **2001**.